PROCEEDINGS OF ECOS 2023 - THE 36TH INTERNATIONAL CONFERENCE ON
EFFICIENCY, COST, OPTIMIZATION, SIMULATION AND ENVIRONMENTAL IMPACT OF ENERGY SYSTEMS
25-30 JUNE 2023, LAS PALMAS DE GRAN CANARIA, SPAIN

Innovative thermal management operating strategies for battery-electric heavy-duty trucks

Jan Friedrich Hellmuth[a], Michael Steeb[a], Markus Pollak[a], Florian Jäger[a], Wilhelm Tegethoff[a,b] and Jürgen Köhler[a]

[a] Technische Universtität Braunschweig, Germany, jan.hellmuth@tu-braunschweig.de
[b] TLK-Thermo GmbH, Braunschweig, Germany

Abstract:

Thermal management systems of electrified vehicles especially heavy-duty trucks face multiple competing goals such as minimum energy consumption, minimum battery degradation and highest passenger comfort. The design process of a suitable thermal management system addressing these goals requires a holistic approach including the various cross couplings occurring in real world operation. Therefore, a physics-based modular full-vehicle model is introduced. The model includes an electrified drive-train, passenger cabin and thermal management system. The mechanical and electrical drive-train components, including the battery, motor and power electronics are thermally connected with each other and the cabin using various cooling circuits. A reversible heat pump and several control units are used to adjust the specific thermal requirements leading to complex interconnections and cross couplings. We estimate the performance of a heavy-duty truck on typical long-distance trips including stops based on legal regulations used for fast charging and overnight charging. While charging overnight, conservation air conditioning of the cabin is performed as efficiently as possible. For this operation, we present different strategies for battery thermal conditioning. Operating strategies for the full vehicle, especially the thermal systems in a summer and a winter scenario are proposed. Simulations of a typical deployment scenario are performed to explore the effects of different operating and control strategies for thermal management. Our virtual deployment scenarios include easy to modify driving cycles, driving time regulations, charge stops and climatic boundary conditions. For evaluation purposes we present an energy-flow-diagram for the full vehicle. Based on the simulation results we recommend thermal system operating strategies in a full-vehicle context for heavy-duty truck long distance trips and charging.

Keywords:

battery, heating, cooling, electric trucks, R744 thermal management, driving range, battery degradation, fast charging.

1. Introduction

In order to fulfill Paris goals for reducing CO_2 emissions in the transport sector, electrically powered trucks are needed. Both, battery-electric or fuel-cell trucks show promise for flexible transport of goods [1]. Some recent investigations discuss opportunities and challenges for fuel-cell trucks [2, 3]. An overview of current long-haul heavy-duty fuel-cell trucks is given by Pardhi et al. [4]. While it is believed that both, battery-electric and fuel-cell technologies will be used to power future heavy-duty trucks [5]. In this research we only focus on battery-electric heavy-duty trucks.

The transformation from internal combustion engines to electrically powered vehicles has occurred rapidly for passenger cars, as observed in car registration statistics of different countries [6]. Although electrical powered trucks became available in recent years [5, 7], the adoption of heavy-duty vehicles has been slow compared to light-duty vehicles [8]. Several reasons for the slower transition can be identified. First, heavy-duty trucks are typically required to cover longer distances than light-duty vehicles, while carrying large amounts of cargo. Therefore, the battery systems suitable for a heavy-duty truck must be much larger compared to that of a light-duty vehicle. Second there is a lack of fast charging stations, especially *MW*-Chargers [9], for trucks along the main transport routes resulting in longer stop times compared to conventionally powered vehicles. Third, electric trucks are still much more expensive than conventional trucks [10] and their diesel engines are already optimized on efficiency [2].

Several investigations found in the literature motivate the current study. Verbruggen et al. [11] performed simulations for powertrain design of a battery-electric heavy-duty truck. Nykvist and Ollson [12] performed an analysis on the feasibility of battery electric heavy-duty trucks and in doing so considered fast-charging and range in their investigation. Several authors investigated thermal behavior of large battery packs suited for trucks, e.g. [13]. Furthermore, the influence of thermal encapsulation of truck batteries was investigated. Energy savings for overnight parking are highlighted [14].

https://doi.org/10.52202/069564-0232

Our study focuses on the choice of operating strategies for the thermal management system of the whole truck during driving and charging, which has not been addressed in the literature. To analyze the effects of different operating strategies on energy consumption, battery degradation and thermal comfort, we model the full vehicle in order to take into account cross couplings. As an extension to the previously published studies we propose to employ a detailed physics-based model to investigate battery-electric trucks. With our approach a detailed analysis of the entire vehicle and its subsystems is possible. Furthermore, we describe the degradation of the battery, which allows us to predict the overall lifetime of the truck. Our model also allows different vehicle configurations to be tested. Furthermore, sensitivity analysis for certain parameters can be performed and parameters can be optimized easily.

Our physics-based vehicle model (see figure 2.) accounts for all the main components of a battery-electric heavy-duty truck with a special focus on the details of the thermal systems. The truck uses a state-of-the art Li-Ion battery system designed for performing long-distance trips with full payload. Our system contains NMC-Pouch cells [12]. Other manufacturers plan to use LFP cells [15]. In the future, solid state batteries may also be used for heavy duty trucks [16]. Electric and mechanical components such as motors, power electronics and gears produce waste heat [17]. Our model accounts for this waste heat and also includes battery degradation, which increases significantly at operating temperatures that are either too high or too low [18, 19]. During fast-charging battery waste heat can be very high [20]. Additionally, there is a need for cabin air conditioning and a fresh air supply.

As a result of these points, there is a need for a multi-function thermal management system. Because a long driving range is a main requirement for heavy-duty trucks, the thermal management should be as efficient as possible [21]. Different operating strategies can be applied [22] to optimize energy consumption. Also, battery degradation in the context of a full truck and different environments and operating conditions can be investigated because of the implemented degradation model [18].

We employed test scenarios with challenging conditions for the analysis of the whole system of a battery-electric heavy-duty truck. Operating strategies are compared in terms of battery degradation and energy consumption. Long-distance trips are the most challenging deployment scenario for battery-electric vehicles [23] and therefore, we focus especially on these long-distance trips. There is a need for large battery capacities and rapid charging [5] to minimize break times. In a parameter study, the effects of different boundary conditions as well as operating strategies on the aforementioned energy consumption, battery degradation and thermal comfort are investigated. The boundary conditions include harsh climatic conditions such as very high or low temperatures that are challenging [14, 24], due to the increased energy demands for thermal management. Furthermore, the driving cycle could be challenging, especially for hilly terrain. Due to the large weight of a typical battery-electric truck, which can weigh as much as 42 metric tons [24], high rolling resistances and grade resistances occur. For downhill driving, significant recuperation is possible, which can reduce energy consumption but results in higher loads for the mechanic and electric components and more waste heat. Simulations of the battery-electric truck on different trips using different operating strategies are conducted and investigated. The effects of the different operating strategies on the behavior of the system are analyzed in detail.

2. Description of the Modular Full Vehicle Model

For our investigations we use a modular multi-scale vehicle model implemented in Modelica modelling language using models from the TIL suites [25]. Due to its modular structure, the model can be configured for different types of vehicles such as busses, heavy-duty trucks or passenger cars. An earlier version of the model was presented by Steeb et al. [26]. They combined the vehicle model with a high-dimensional battery model and investigated thermal hotspots in automotive batteries.

A block diagram of the vehicle model used in this study is shown in figure 1. The model in general can be structured into mechanical, electrical and thermal sub-models. Furthermore, the model includes boundary conditions and control units for several models.

The boundary conditions (described in details in section 3.) include climate data and a drive cycle. We set the ambient temperature,ambient humidity and solar radiation as climate conditions. These affect the driving resistance and, importantly, act as the boundary conditions for all thermal models, having particular influence on the cabin, cooling circuit, and the reversible heat pump (RHP).

The drive cycle provides time-based calculated data for the vehicle's velocity and slope. We took distance-based data and re-calculated those for use in a time-based calculation. The time-based format fits well into the overall solution process of the formulated system of equations. For example, time-based driver rest stops can be set easily. Also, for heavy-duty trucks, the payload can be varied, and a time-based format enables the payload to be modified during a multi-stage trip. Furthermore, the drive cycle can set a charging request if ignition is activated. A driver model compares target speed with actual speed. Target speed is set as a boundary condition by the drive cycle. The driver is designed as a controller calculating brake or acceleration

pedal position. Data for slope and payload are processed in the driving resistance.

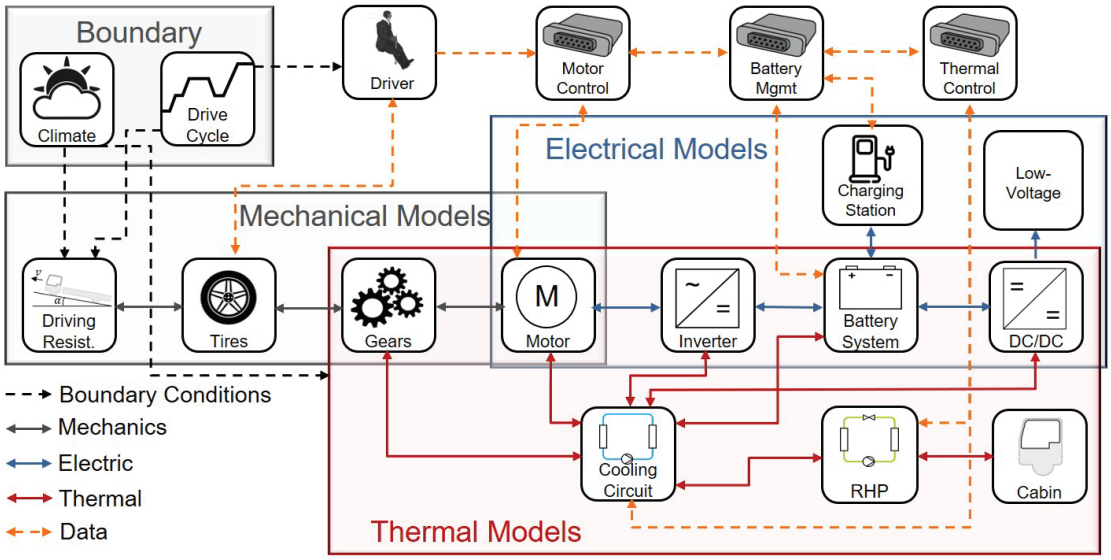

Figure 1: Model of a full vehicle including balance rooms for flow variables (mechanical and electrical power, heat), data connection , and boundary conditions, adapted from [26].

2.1. Models of Mechanical Drive-train and Force Components

The mechanic part includes models for driving resistance, tires, gears and an electric motor describing the driving dynamics of a configured vehicle. The driving resistance model includes replaceable parameter sets for drag coefficient c_w, frontal area A_{front}, weight $m_{vehicle}$ and rolling friction coefficient μ_{roll}. These values are summarized in Table 1. Traction force is calculated by summing roll, air, grade and acceleration resistance:

$$F_{Traction} = F_{Roll} + F_{Air} + F_{Grade} + F_{Acceleration} \tag{1}$$

Rolling resistance F_{Roll} and grade resistance F_{Grade} mainly depend on the vehicle mass $m_{vehicle}$ and rolling friction coefficient μ_{roll}. Air resistance F_{Air} is influenced by the frontal area A_{front} and drag coefficient c_w. The driving resistance model receives slope and the additional vehicle weight due to payload from the driving cycle model.

Table 1: Vehicle parameters used in all scenarios.

Vehicle total mass	Frontal area	Drag coefficient	Rolling friction coefficient
42 t	9.25 m^2	0.5	0.0055

The tires convert torque from gears into translational movements $F_{Traction}$ of the vehicle on the street (driving resistance model). The tire model also takes into account braking force and the tire inertia. Vehicle velocity and distance are calculated. Data are shared into a data-bus system. The gears model mechanically connects the tires and electrical motor. It operates at a constant efficiency and conserves inertia. Constant efficiency means that the incoming power is divided into a mechanical fraction, which is passed to the drive train, and heat. A thermal model is included in the gear model and accounts for waste heat rejected to the cooling circuit.

The electric motor is modeled with a fixed efficiency as well. The model includes replaceable data sets for motor characteristics such as torque data or inertia. The motor torque set-point is provided by the motor control unit. That translates the brake or acceleration pedal positions into motor torque. Constraints are taken into account including battery management data such as minimum recuperation temperature, maximum charging or discharging power, and motor limits. The motor provides mechanical power P_{mech} to the tires and calculates thermal losses P_{loss}.

2.2. Models of Electrical Components

The motor model acts as an interface to the mechanical and electrical models. The needed electric power P_{el} is calculated as the sum of P_{mech} and P_{loss}. While the motor operates at a constant voltage the electric

https://doi.org/10.52202/069564-0232

current depends on P_{el}. An inverter model provides electric power at a constant voltage level. It also operates at a constant efficiency. The inverter model is electrically connected to the battery system including a high voltage network. Furthermore, the DCDC-Converter enables a connection to a low voltage network. The low voltage network provides power for energy consumers such as ignition or infotainment. A charging station model is included. The charging can be activated by the station itself for time-based charging, or requested by the drive cycle. Charging power is controlled by the battery management. We implemented state-of-the-art charge maps that provide feasible charging powers depending on the actual battery temperature and its state of charge (SoC). Furthermore, a derating of charging power for high battery temperatures is applied.

The Li-Ion battery system is the key component of a battery-electric vehicle (BEV) and, therefore is modeled with many details [22, 26]. The battery system consists of a cooling plate, a thermal interface material and of a typical pouch cell with a nominal capacity C_N, as well as current arresters. On the battery system level, we model one representative battery cell and scale current, voltage and heat exchange up to system level. The battery system is designed for an on-board supply voltage of $800\,V$ and has a battery capacity of $725 kWh$. The representative single battery cell is modeled with a 2-dimensional (length and height) discretized model using thermally and electrically connected battery bundles. A battery bundle represents a single discretized part of a battery cell including the same behavior and equations for the adjusted cell volume, mass and capacity [27]. Each battery bundle includes an equivalent circuit model for electric modeling and calculating irreversible ($\dot{Q}_{irrev}$) and reversible ($\dot{Q}_{rev}$) heat production [28]:

$$\dot{Q}_{irrev} = R_i \cdot I^2 \tag{2}$$

$$\dot{Q}_{rev} = I \cdot T \cdot \frac{\partial U_{OCV}(T, SoC)}{\partial T} \tag{3}$$

The internal resistance $R_i(SoC, T)$ depends on temperature T and SoC. Irreversible heat production grows quadratic with higher currents, while the internal resistance typically decreases with higher temperatures. Reversible heat can be positive or negative. For high currents, its effect is small compared to $\dot{Q}_{irrev}$.

For State of Health (SoH) calculations, a semi-empirical battery degradation model based on the investigations of Wang et al. [18] was implemented. The SoH depends linearly on Ah-throughput $Ah_{Throughput}$, exponentially on the C-Rate, defined as $c\text{-}Rate = I/C_N$, and an Arrhenius-Term is used to describe the temperature dependence. Since the model is valid for a wide temperature and C-Rate range, it is capable of capturing the temperature and C-Rate coupling. Therefore, optimal thermal operating points for a given electric stress can be derived from the model. For moderate C-Rates, the optimum temperature of $25^\circ C$ results in the lowest degradation rate while higher and lower temperatures cause the degradation rate to increase rapidly. Other degradation dependencies like depth of discharge or SoC are neglected, which is a reasonable assumption due to the almost stationary use-case-scenarios of heavy-duty trucks. As outlined by [29], the chosen model seems to be the most suitable for the considered application. The model is valid for a wide temperature and C-Rate range. It is capable to describe the coupling of temperature and C-Rate. Optimal thermal operating points for given electric stress can be identified with an equation for ΔSoH depending on T, C-Rate and fitting parameters $a-e$:

$$\Delta SoH = (a \cdot T^2 + b \cdot T + c) \cdot \exp(d \cdot T + e) \cdot C-rate \cdot Ah_{Throughput} \tag{4}$$

2.3. Models of Thermal Components

As described previously, models of the gears, motor inverter and DCDC-Converter use thermal sub-models. The thermal sub-models contain the waste heat production as well as thermal capacitors and resistors describing the geometry and thermal behavior. Motor, gears and inverter thermally interact with the environment and the liquid cooling circuit. Similarly, battery cooling is connected to the cooling circuit. We use a cooling plate model for calculating convective and conductive heat transfer from liquid to the battery cells.

The cooling circuit model (see Figure 2; liquid) includes the interface to the ambient air that flows through the front-end heat exchanger of the truck. A fan is used to increase the air flow rate across this heat exchanger. Each of the two liquid loops are equipped with an air-liquid heat exchanger that is used for heat rejection to the ambient. A low temperature loop is designed for battery cooling. A high temperature liquid loop is used for cooling of motor, gears and inverter. Both cooling circuits use liquid pumps and for certain use cases, connections of the circuits are possible (e.g. battery heating).

Figure 2 depicts a piping and instrumentation diagram of the reversible heat pump with continuous lines marking the activated cooling mode. A third heat exchanger on the air path located in the front-end of the vehicle is used as an evaporator or gascooler/condenser in the reversible heat pump. It is designed as a two-stage R744-refrigeration cycle with switchable operation modes enabling heating or cooling of the battery and cabin. The refrigerant flows through the compressor and enters at a high pressure level in the *Gascooler*, which is bypassed on the air side. Next the refrigerant flows through the open *Valve 1*. Gascooling takes place in the

Front-End HX (heat exchanger) and the *Internal HX*. After that the refrigerant mass flow is divided to provide battery and cabin cooling. In the battery path refrigerant flows through *Valve 3* and is expanded in *Valve 4*. The R744 is evaporated in the *Battery HX* cooling the liquid coolant used for battery cooling. After that the refrigerant flows through *Valve 7* and *Valve 8*. For cabin cooling the refrigerant is expanded in *Valve 5* and flows through *Valve 6* and into the Evaporator, conditioning the fresh air for cabin cooling. Both refrigerant flows get mixed and enter the *Accumulator* and the the low pressure side of the *Internal HX*. Both, the RHP

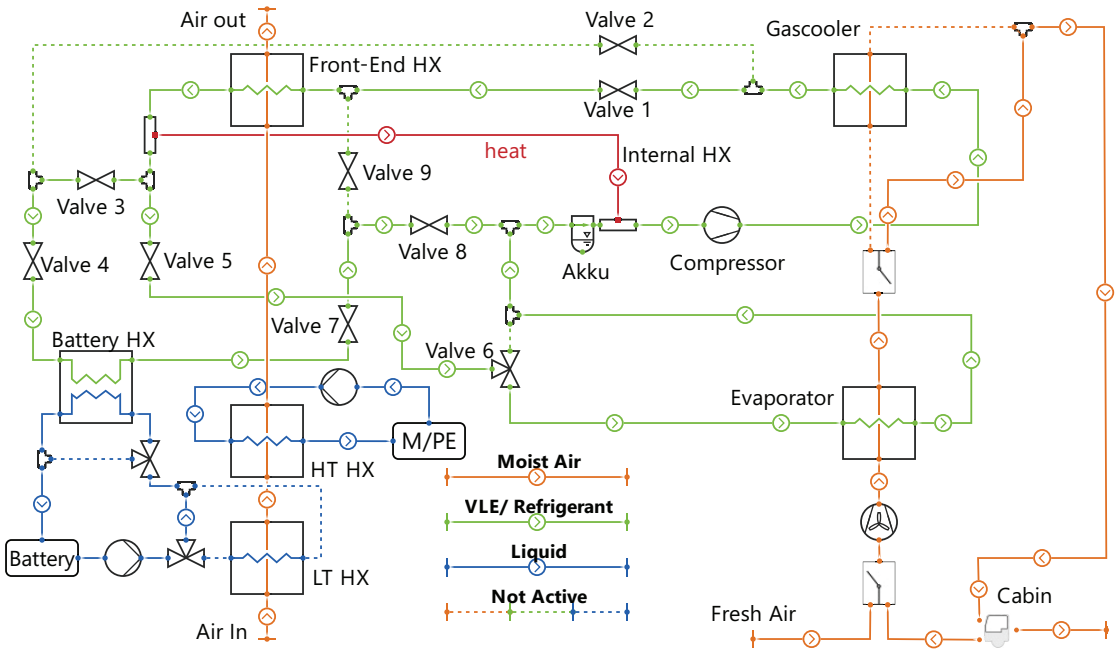

Figure 2: Piping and Instrumentation Diagram with TIL components of a reversible heat pump for cooling and heating of battery and cabin and the simplified cooling circuits including cooling of electric motor (M) and power electronics (PE). The case of the battery and cabin cooling is displayed.

and cooling circuit exchange data with a thermal control unit that specifies setpoint temperatures depending on the actual state of the vehicle and its subsystems. We use sets of PI-controllers for implementing different control strategies.

As described previously, the reversible heat pump is used for conditioning the vehicle cabin. The cabin interacts with the boundary conditions: Ambient temperature and humidity, solar radiation and driving speed. For simplicity, we always set $22°C$ as our target temperature for cabin air.

3. Deployment Scenarios and boundary conditions

We present two typical driving cycles each paired with two climatic conditions resulting in challenging deployment scenarios for a heavy-duty truck. These scenarios are used to investigate the effects of different operating strategies on the defined performance metrics. The applied operating strategies are discussed in the next section. The first drive cycle represents a typical long-distance day-trip for a truck in Germany and is depicted in Fig. 3. Starting in Hanover, the truck travels the 632 km distance to Munich in about 8 hours and 10 minutes excluding stops. The truck starts the drive cycle with half an hour of pre-conditioning followed directly by four and a half hours of mostly full-speed *Autobahn*-Driving. Due to regulations, a break of 45 minutes is required after that time. This break is also used for fast charging. Fast charging during the stop is required to cover the remaining driving distance for the day. For our analysis, the route is driven in a summer scenario with an outside temperature of $35°C$ and a high solar radiation affecting the truck's cabin.

Second, we investigate a two-day long distance trip. The two-day cycle is designed as a simplified driving cycle according to the maximum allowed driver's steering time in European Union regulations [31]. The whole trip runs for 1530 km on a flat terrain. Such a trip could be seen as a trans national European drive from Lithuania to Belgium. The velocity profile including pre-conditioning and rest (and charge) breaks can be seen in Figure 4. The tour starts with 3 hours of pre-conditioning, followed by two consecutive four and a half hour driving periods at $85\frac{km}{h}$ interrupted by a 45 minute resting and charging break. The night break is 11 hours and then

https://doi.org/10.52202/069564-0232

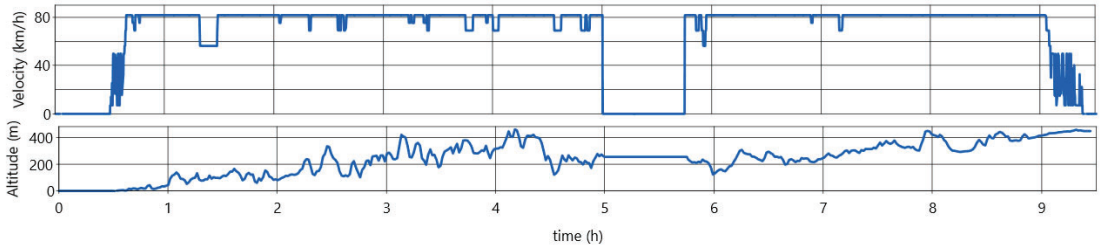

Figure 3: Hanover-Munich long-distance day-trip: Velocity and Altitude profile with rest and fast charging break, adapted from [30].

the same procedure will be driven the second day. During the short breaks fast charging will be performed. Slow charging is performed during the night break. During all charging breaks, cabin air conditioning must be provided.

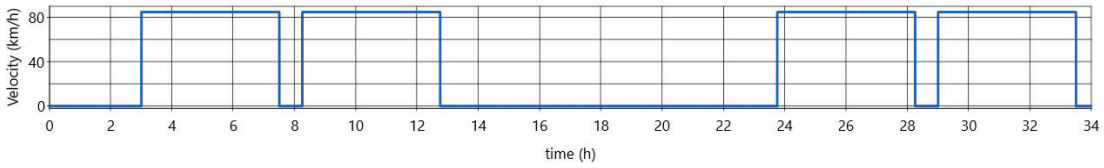

Figure 4: Velocity profile for a two-day long distance trip without altitude changes, including two fast charging brakes and one overnight brake.

4. Operating Strategies

An operating strategy is needed to handle competing goals pertaining to thermal management in the vehicle's operation. Those goals include:

- Minimum battery degradation
- Best thermal comfort for the driver
- Minimum energy consumption and maximum driving range

These goals are constrained by the following additional conditions: Safe operation of all vehicle components and systems, especially the battery and reaching suitable charging times. Most of these goals are in competition at various points of operation and must therefore be prioritized. Battery degradation can be reduced by maintaining optimum battery temperature and operating at low C-Rates. Maintaining suitable battery temperature, increasing energy consumption reduces driving range. If the reversible heat pump is working, a strategy for cooling or heating priority between the cabin and battery is necessary.

Two operation strategies for the summer scenario Hanover-Munich trip are suggested. One strategy prioritizes **minimum energy consumption**. The other strategy prioritizes **minimum battery degradation**. For safety reasons, thermal comfort of the driver is always prioritized and the best possible comfort is provided. For the **minimum battery degradation** strategy, the thermal system tries to cool the battery as much as possible to quickly reach and maintain the degradation-minimizing temperature. This is especially important during and after fast charging. For minimum energy consumption strategy, less intense battery cooling is performed at a more optimal operating point of the RHP and the target temperature for battery cooling is set higher than the degradation-minimizing temperature to save energy in thermal management.

Two operation strategies for fast charging during the two-day long-distance trip are suggested. We distinguish between a 45 minute daytime charging break that satisfies legal requirements, and lengthening the day-time charging breaks by 15 minutes resulting in a total of 30 minutes longer trip time. Minimum charging time competes with minimum battery degradation, which is expected to be higher when higher charging power is used.

In winter scenario we investigate the influence of battery pre-conditioning based on the two-day long distance trip. We compare different target temperatures for battery heating by the reversible heat pump during an hour of pre-conditioning before driving on a flat terrain for 9 hours including a fast-charging brake of 45 minutes.

https://doi.org/10.52202/069564-0232

The winter scenario also includes fast charging breaks but due to lower ambient temperatures battery cooling is easier. During overnight charging a constant heating and fresh air supply for cabin are required. For overnight charging, we study an eight hour night-time break for charging. The truck arrives with a nearly empty battery (SoC = 10%) and charges with a constant charging power (P_{charge} = 75 kW). We distinguish three thermal management operating strategies for RHP operation (see figure 2) during overnight charging. Our first strategy uses battery waste heat as the heat source for RHP, forming a water-air heat pump. Due to the relatively high temperature level and capacity of the battery a very high heating efficiency is expected. The second strategy utilises ambient air as heat source forming a typical air-air heat pump. Finally, the third strategy uses an electric heater. It is used as a benchmark for comparison of the electrical energy consumption and possible savings.

5. Results

To analyze cross couplings in the complex system that is the full truck model, we use a energy-flow diagram on the top level. Figure 5 shows the flow rates of the three main process variables: Mechanical and electrical power as well as heat flow rates. The diagram shows a summer case at an ambient temperature of 35°*C* and the Hanover-Munich route. The current and average consumption of electrical energy an other simulation parameters are depicted, cf. Fig 5. At the moment of the operational snapshot in Figure 5 the truck is climbing

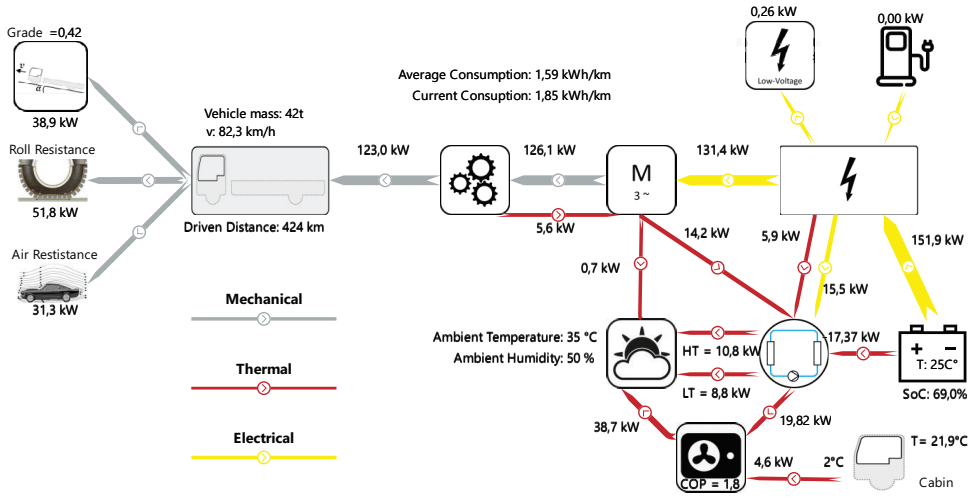

Figure 5: Energy flow diagram showing the mechanical, electrical and thermal power flows and additional information about the vehicle state an hour after fast charging in the Hanover-Munich cycle.

a slight grade. Efficiencies of sub models (e.g. gears) can be observed from the different powers displayed at each side of the component. Thermal and mechanical inertia of the components are included. The battery rejects 17.37 kW of heat to the cooling system. Heat is released to the cooling cycle and a small portion directly to the environment by the LT-Cooler and partly to RHP. Cabin cooling is also performed through RHP on a lower temperature level.

5.1. Model Plausibility Check

We checked the plausibility of our heavy-duty truck model by comparing it to test data available for the *Volvo FH Electric* [10], which is a battery-electric truck of the same class as the one that was modelled. The real world test of the Volvo truck resulted in an average energy consumption of 1.1 $\frac{kWh}{km}$ for a 338 km route with a diverse topography in Southern Germany [10]. We took the same route and chose a summer scenario with an ambient temperature of 28°*C* to investigate the modelled truck. Cabin cooling is performed to keep the cabin at 22°*C*. Our simulation resulted in an average energy consumption of 1.33 $\frac{kWh}{km}$. The 21% difference in the results can possibly be attributed to differences in the energy consumption for air conditioning, the truck's weight or slightly different roll and air resistances.

5.2. Influence of Thermal Management Operation Strategy for Summer Scenario

In Figure 6, the comparison of battery degradation, represented as the change in SoH and battery temperature for the Hanover-Munich trip in summer is shown for both operation strategies (see section 4.). The degradation is reduced by 40% when applying the **minimum battery degradation** operating strategy compared to the

https://doi.org/10.52202/069564-0232

minimum energy consumption strategy. On the other hand, at the beginning of fast charging at a time of 5 hours, 2.3% percent of SoC or 9 kWh of energy is saved for **minimum energy consumption** operating strategy.

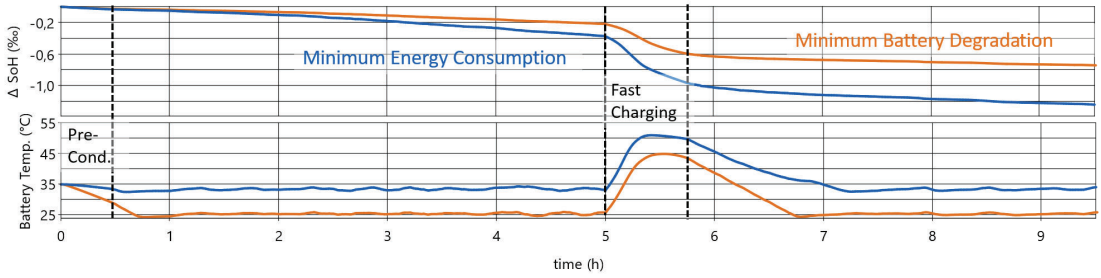

Figure 6: SoH degradation and battery temperature for a Hanover-Munich long distance day trip on challenging topology and two operation strategies: **minimum battery degradation** (orange) and **minimum energy consumption** (blue). Battery degradation is reduced by 40% using the **minimum battery degradation** operating strategy.

This investigation underlines the trade-off between energy consumption for thermal conditioning of batteries and battery degradation. Because only small energy savings are achieved with the **minimum energy consumption** strategy compared to the driving energy but large difference in battery degradation is observed using the **minimum battery degradation** strategy. Preference should be given to battery cooling to limit degradation.

5.3. Influence of Fast Charging Strategies on Long Distance Trips

We investigate the influence of fast charging on battery degradation incorporated in a long distance trip (see Figure 4.To do this we lenghtend the charging break from 45 minutes to 60 minutes and reduced the associated charging power by 25%. Figure 7 illustrates the differences in battery degradation for the two fast charging times over the whole two day trip.

First, this investigation shows the enormous influence of fast charging operation on battery life, which can be seen by comparing the blue and orange curves in Fig. 7. It can be seen that battery degradation during charging is significantly higher than while driving. This results from the larger currents that occur during fast charging compared to the discharging currents drawn from the battery while driving. Also the battery is facing those higher currents at higher temperature levels which is another crucial factor for the degradation.

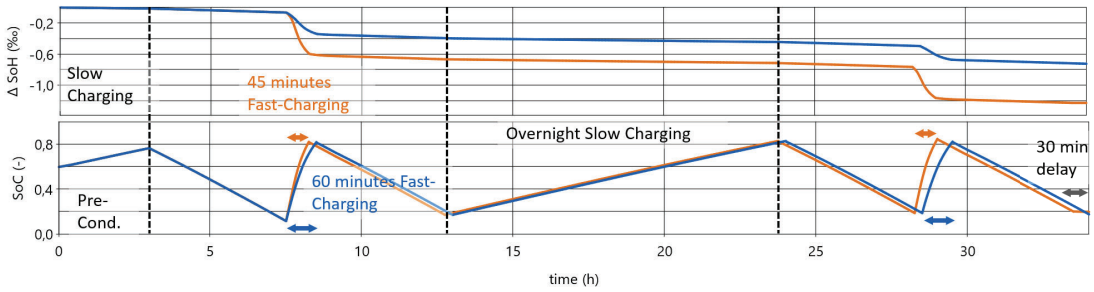

Figure 7: SoH degradation and SoC over a two-day long distance trip with two operating strategies for daily fast charging: 45 minute charging breaks (orange), extended 1 hour charging breaks (blue). Significant reductions (42%) in battery degradation are seen for longer charging breaks.

Second, Fig. 7 shows the effect of lengthening charging breaks by 15 minutes and at the same time reducing charging power on battery degradation. By extending the break time by 15 minutes, resulting in an additional 30 minutes beeing needed for the two-day trip, the battery degradation can be reduced by 42%. Further elaboration is recommended to analyze the economical trade-off between battery degradation and depreciation and delivery time. The preliminary discussed goals of fast charging time and battery degradation conflict strongly.

The results of this investigation enable us to approximate the total battery lifetime expectancy. Driving the two-

day long distance trip, the battery looses 0.07% of its state of health when taking 60 minute charging breaks. By extrapolating the result down to a SoH of 80%, a battery lifetime of 287 drive cycles or 437.000 *km* is approximated. Considering the result for the same drive cycle but using 45 minutes charging breaks a lifetime range of only 245.000 *km* can be achieved. This result confirms that battery change could be necessary during the lifetime of the truck, particularly if fast charging is performed regularly. A separate depreciation of the battery and other components is suggested, and battery degradation should be considered in logistics operation strategies.

5.4. Influence of Terrain on Battery Degradation

To asses the influence of terrain, we compare the Hanover-Munich trip (Fig. 6) to the long distance trip (Fig. 7) for total trip battery degradation. Although the long-distance trip is more than 2.42 times longer than the Hanover-Munich trip, the battery degradation is similar. This directly translates to a higher degradation per unit distance driven for the Hanover-Munich cycle. The effect can be explained by the challenging terrain of the Hanover-Munich cycle that results in much higher discharging C-Rates for hill climbing and recuperation when going downhill. When combined, these effects lead to a higher total number of battery charging and discharging cycles.

5.5. Influence of Battery Aging on Long-Distance Feasibility

To assess the impact of battery aging, we compare previous results for the Hanover-Munich trip for the summer scenario with the same conditions and an already degraded battery. Figure 8 shows a comparison of SoCs against the driving time for a new battery and a degraded battery with a SoH of 0.9. Due to the degradation, not only is the total battery capacity decreased, but the internal resistances are also increased, resulting in more irreversible heat production during charging and discharging. This puts an additional load on the cooling system. The truck reaches the fast charging stop with an SoC of 0.09 instead of 0.19 for a new battery. More intense fast charging needs to be performed, or the charging break needs to be extended, if the truck is required to cover the remaining drive cycle without another stop.

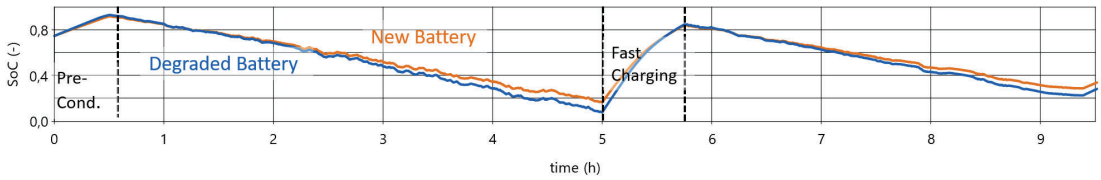

Figure 8: SoC over Hanover-Munich long distance day trip compared for new (orange) and degraded (SoH = 0.9, blue) battery. Less driving range and more intense fast charging result, for the degraded battery.

Our investigations indicate that the loss of battery capacity due to degradation should be taken into account when choosing an appropriate size of battery system for the given operational and range requirements of the vehicle. This again highlights the importance of appropriate thermal management operation strategies to reduce battery degradation.

5.6. Influence of Pre-Conditioning in Winter Scenario

For a one-day long distance trip we compare the influence of pre-heating in a winter scenario at $-5°C$ ambient temperature. After pre-conditioning the battery is heated using waste heat from the motor and electronics as well as its own produced heat.

From figure 9 it can be observed that in a winter scenario battery heating in the pre-conditioning phase can reduce battery degradation significantly. A battery heated to $10°C$ instead of $0°C$ through pre-conditioning reduces battery degradation caused in the first hours of the driving cycle by 33%. Pre-heating the battery up to $20°C$ (which takes more than one hour) does not reduce battery degradation much further. It is demonstrated that operating at low battery temperatures results in accelerated degradation. Battery heating before driving is strongly recommended in winter scenarios. A heat pump is suggested for this purpose to improve energy efficiency.

5.7. Overnight Charging in Winter Scenario

The energy consumption of the three different operation strategies for thermal management for an overnight cabin heating and simultaneous battery charging are displayed in table 2.

The results show, that a heat pump can reduce energy consumption for cabin heating significantly. For 8 hours of overnight cabin heating at an ambient temperature level of $-5°C$, 11.1 kWh of energy are saved using an air-air heat pump instead of an electric heater. Futher saving can be realized by employing the RHP

https://doi.org/10.52202/069564-0232

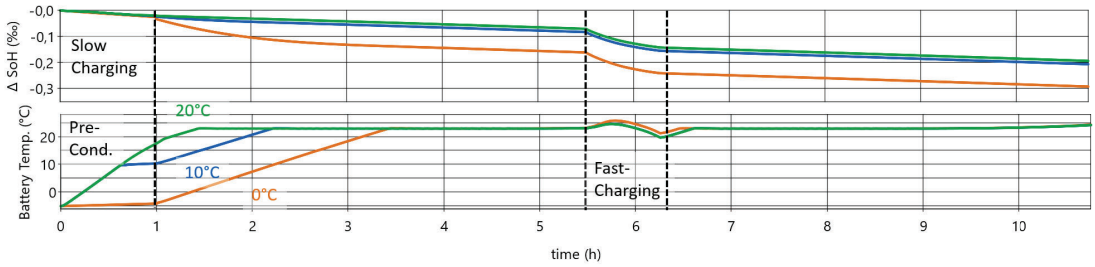

Figure 9: Influence of battery pre-conditioning (with RHP) before driving in a winter scenario with an ambient temperature of -5°*C*. Comparison on battery degradation and battery temperature. Target temperatures for battery heating while pre-conditioning is active: 0°*C* (orange), 10°*C* (blue), 20°*C* (green).

Table 2: Electric energy consumption of different cabin conservation air conditioning thermal management strategies (see section 4.) during overnight charging in winter scenarios.

Water-Air Heat Pump	Air-Air Heat Pump	Electric Heater
2 kWh	3.9 kWh	15 kWh

(see figure 2) as an water-air heat pump during overnight charging. The electrical energy consumption could be halved again for this operation strategy. When using the water-air heat pump only the *battery HX* and *gascooler* transfer heat. During overnight slow-charging the battery waste heat is efficiently used as RHP heat source. Depending on the chosen charging speed, the current SoC, the SoH of the battery and the ambient temperature the waste heat approximately covers the required heat for RHP. If the predicted demand of heat to keep the cabin temperatured exceeds the amount of available waste heat of the battery, that is produced while charging the battery, the battery could also be used as a thermal capacity. Therefore, battery operating temperature could be increased during the last hours of operation before overnight break in order to have a higher temperature level of the RHP heat source. After that battery temperature could slowly be decreased overnight using battery as heat source for RHP.

6. Conclusions and Outlook

In our study, we demonstrated that a physics-based full-vehicle model of a battery-electric truck is suitable to accurately predict the consumption of electrical energy in a benchmark scenario. Using the full-vehicle model, the effect of fast charging on the state-of-health of the battery was explored using real-world deployment scenarios. It was found that fast charging stops have an important impact on the achievable life time of a battery electric truck.

Our study also compared different operating strategies for summer and winter scenarios. Fast-charging breaks along with legally required minimum break time leads to accelerated battery degradation. A slight extension of charging times and associated lower charging currents lead to significantly less battery degradation and thus much less depreciation on the battery (truck). Prioritizing minimum battery degradation over minimum energy consumption as thermal management operating strategy leads to significant reduction in battery degradation.

Furthermore, our investigations showed how a challenging hilly terrain influences battery degradation due to high discharge currents while driving uphill and high charging currents for recuperating while driving downhill. In this context we exemplary contrasted the remaining capacity when reaching predefined charging stops of a pristine and a degraded battery to evaluate the long-distance feasibility over lifetime. The results showed that especially for long-haul trucks the battery size should be designed anticipating degradation due to aging. For the investigated winter scenario we showed the positive effect of pre-heating the battery before driving. Pre-heating lowers degradation significantly. For battery and cabin heating a heat pump is recommended due to energy efficiency. For overnight heating operation the heat pump is used as well. Battery waste heat while slow charging can be used as a heat source for an efficient heat pump.

Looking to the future, solid state batteries are a promising development in battery technology. It is predicted that they will require a higher temperature level for operation [16]. For long distances and driving times of heavy-duty trucks, as well as route planning and pre-conditioning times, solid-state batteries are especially suitable for trucks. Adjusted thermal management systems are needed with solid state batteries. There is a special need for heating technologies and battery pre-conditioning. Due to its modular structure, our model is well suited for such investigations in the future.

https://doi.org/10.52202/069564-0232

Acknowledgments

As this work was funded under grants AUTO-GEN (01IS20086B) and PHYMOS (19I20022I), the authors would like to thank the German Federal Ministry of Education and Research and the German Federal Ministry of Economic Affairs and Climate Action for their financial support.

References

[1] Camacho, María de las Nieves, D. Jurburg, and M. Tanco, "Hydrogen fuel cell heavy-duty trucks: Review of main research topics," International Journal of Hydrogen Energy, vol. 47, no. 68, pp. 29505–29525, 2022, https://doi.org/10.1016/j.ijhydene.2022.06.271.

[2] Wagenblast, M., Pollak, M., Trägner, J., Heinke, S., Tegethoff, W., Köhler, J., Swoboda, J.,*Design and Analysis of a Spray Cooling System for a Heavy-Duty Fuel Cell Truck*. SAE Technical Papers 2022 2022-01-5054 https://doi.org/10.4271/2022-01-5054

[3] Cullen, D. and Neyerlin, K.C. and Ahluwalia, R. and Mukundan, R. and More, K. L. and Borup, R. L. and Weber, A. and Myers, D. and Kusoglu, A.,*New roads and challenges for fuel cells in heavy-duty transportation*. Nature energy 2021;6:462–474.

[4] S. Pardhi, S. Chakraborty, D.-D. Tran, M. El Baghdadi, S. Wilkins, and O. Hegazy, "A Review of Fuel Cell Powertrains for Long-Haul Heavy-Duty Vehicles: Technology, Hydrogen, Energy and Thermal Management Solutions," Energies, vol. 15, no. 24, p. 9557, 2022, https://doi.org/10.3390/en15249557.

[5] NOW GmbH, Nationale Organisation Wasserstoff- und Brennstoffzellentechnologie, "Marktentwicklung klimafreundlicher Technologien im schweren Straßengüterverkehr: Auswertung der Cleanroom-Gespräche 2022 mit Nutzfahrzeugherstellern," 2023.

[6] IEA, Electric car registrations and sales share in selected countries, 2016-2021;Charts – Data & Statistics - IEA. [Online]. Available: https://www.iea.org/data-and-statistics/charts/electric-car-registrations-and-sales-share-in-selected-countries-2016-2021 (accessed: Feb. 24 2023).

[7] S. Bhardwaj and H. Mostofi, "Technical and Business Aspects of Battery Electric Trucks—A Systematic Review," Future Transportation, vol. 2, no. 2, pp. 382–401, 2022, https://doi.org/10.3390/futuretransp2020021.

[8] M. Muratori et al., "The rise of electric vehicles—2020 status and future expectations," Prog. Energy, vol. 3, no. 2, p. 22002, 2021, https://doi.org/10.1088/2516-1083/be0ad.

[9] W. Shoman, S. Yeh, F. Sprei, P. Plötz, and D. Speth, "Public charging requirements for battery electric long-haul trucks in Europe: A trip chain approach," 2023.

[10] Volvo FH Electric — Testbericht Trucker 2022-01. [Online]. Available: https://brochures.volvotrucks.com/de/volvo-trucks/testberichte/2022/volvo-fh-electric-testbericht-trucker-2022-01/?page=10 (accessed: Feb. 24 2023).

[11] F. Verbruggen, V. Rangarajan, and T. Hofman, "Powertrain design optimization for a battery electric heavy-duty truck," in 2019 American Control Conference (ACC), Philadelphia, PA, USA, 2019, pp. 1488–1493, https://doi.org/10.23919/ACC.2019.8814771.

[12] B. Nykvist and O. Olsson, "The feasibility of heavy battery electric trucks," Joule, vol. 5, no. 4, pp. 901–913, 2021, https://doi.org/10.1016/j.joule.2021.03.007.

[13] A. Ramesh Babu, J. Andric, B. Minovski, and S. Sebben, "System-Level Modeling and Thermal Simulations of Large Battery Packs for Electric Trucks," Energies, vol. 14, no. 16, p. 4796, 2021, https://doi.org/10.3390/en14164796.

[14] A. Ramesh Babu, B. Minovski, and S. Sebben, "Thermal encapsulation of large battery packs for electric vehicles operating in cold climate," Applied Thermal Engineering, vol. 212, p. 118548, 2022, https://doi.org/10.1016/j.applthermaleng.2022.118548.

[15] L. Leicht, "Mercedes E-Actros Long Haul," 18 Sep., 2022. https://www.auto-motor-und-sport.de/elektroauto/mercedes-e-actros-long-haul-elektro-lkw-fuer-den-fernverkehr/(accessed: Mar. 2 2023).

https://doi.org/10.52202/069564-0232

[16] R. Hughes and C. Vagg, “Assessing the Feasibility of a Cold Start Procedure for Solid State Batteries in Automotive Applications,” Batteries, vol. 8, no. 2, p. 13, 2022, https://doi.org/10.3390/batteries8020013.

[17] F. Liu, M. Li, B. Han, J. Guo, and Y. Xu, “Research on integrated thermal management system for electric vehicle,” Proceedings of the Institution of Mechanical Engineers, Part D: Journal of Automobile Engineering, 2022, https://doi.org/10.1177/09544070221114677.

[18] Wang, J. ; Purewal, J. ; Liu, P. ; Hicks-Garner, J. ; Soukazian, S.; Sherman, E. ; Sorenson, A. ; Vu, L. ; Tataria, H.; Verbrugge, M. W.: *Degradation of lithium ion batteries employing graphite negatives and nickel–cobalt–manganese oxide + spinel manganese oxide positives: Part 1, aging mechanisms and life estimation*. Journal of Power Sources 269 (2014), 937–948. https://doi.org/10.1016/j.jpowsour.2014.07.030.

[19] X. Zhang, Z. Li, L. Luo, Y. Fan, and Z. Du, “A review on thermal management of lithium-ion batteries for electric vehicles,” Energy, vol. 238, p. 121652, 2022, https://doi.org/10.1016/j.energy.2021.121652.

[20] A. K. Thakur et al., “Critical Review on Internal and External Battery Thermal Management Systems for Fast Charging Applications,” Advanced Energy Materials, p. 2202944, 2022, https://doi.org/10.1002/aenm.202202944.

[21] V. Mali, R. Saxena, K. Kumar, A. Kalam, and B. Tripathi, “Review on battery thermal management systems for energy-efficient electric vehicles,” Renewable and Sustainable Energy Reviews, vol. 151, p. 111611, 2021, https://doi:10.1016/j.rser.2021.111611..

[22] Hellmuth, J., Steeb, M., Tegethoff, W., Köhler, J.: Thermische Simulation im Gesamtfahrzeugkontext. Werkstoffsymposium 2022, Wolfsburg, 17.-18. Mai 2022.

[23] P. Chakraborty et al., “Addressing the range anxiety of battery electric vehicles with charging en route,” Sci Rep, vol. 12, no. 1, p. 5588, 2022, https://doi.org/10.1038/s41598-022-08942-2.

[24] Basma, Hussein, Rodríguez, Felipe, “Long-haul battery-electric trucks in Europe,” icct, The International Council Of Clean Transportation, Berlin, Feb. 2022.

[25] TLK-Thermo GmbH: TIL Suite Simulates thermal systems. https://www.tlk-thermo.com/index.php/en/software/til-suite [accessed 27.02.2023]

[26] Steeb, M.; Flieger, B.; Tegethoff, W.; Köhler, J.: *Avoiding Thermal Hotspots in Automotive Battery Systems using a Multiscale Full Vehicle Model*. 16th Symposium on Modeling and Experimental Validation of Electrochemical Energy Technologies, Braunschweig, 12.-13. March 2019.

[27] Veth, C.; Dragicevic, D.; Pfister, R.; Arakkan, S.; Merten, C. (2014b): 3D Electro-Thermal Model Approach for the Prediction of Internal State Values in Large-Format Lithium Ion Cells and Its Validation. In: J. Electrochem. Soc. 161 (14), A1943-A1952. https://doi.org/10.1149/2.1201412jes.

[28] D. Bernardi, E. Pawlikowski, and J. Newman, “A General Energy Balance for Battery Systems,” J. Electrochem. Soc., vol. 132, no. 1, pp. 5–12, 1985, https://doi.org/10.1149/1.2113792.

[29] X. Jia, C. Zhang, L. Wang, W. Zhang, and L. Zhang, “Modification of Cycle Life Model for Normal Aging Trajectory Prediction of Lithium-Ion Batteries at Different Temperatures and Discharge Current Rates,” World Electric Vehicle Journal, vol. 13, no. 4, p. 59, 2022, https://doi.org/10.3390/wevj13040059.

[30] Kaiser, C.: *Untersuchungen zur Effizienz- und Leistungssteigerung von Omnibusklimaanlagen*. Dissertation, Technische Universität Braunschweig, 2020 https://leopard.tu-braunschweig.de/receive/dbbs_mods_00068696?q=christian%20kaiser.

[31] Your Europe, EU rules for working in road transport - Your Europe. [Online]. Available: https://europa.eu/youreurope/citizens/work/work-abroad/rules-working-road-transport/index_en.htm (accessed: Feb. 22 2023).